



Exhaustive CoMFA and CoMSIA analyses around different chemical entities: a ligand-based study exploring the affinity and selectivity profiles of 5-HT_{1A} ligands

Sara Guariento, Silvia Franchini, Michele Tonelli, Paola Fossa, Claudia Sorbi, Elena Cichero & Livio Brasili

To cite this article: Sara Guariento, Silvia Franchini, Michele Tonelli, Paola Fossa, Claudia Sorbi, Elena Cichero & Livio Brasili (2017) Exhaustive CoMFA and CoMSIA analyses around different chemical entities: a ligand-based study exploring the affinity and selectivity profiles of 5-HT_{1A} ligands, *Journal of Enzyme Inhibition and Medicinal Chemistry*, 32:1, 214-230, DOI: [10.1080/14756366.2016.1247057](https://doi.org/10.1080/14756366.2016.1247057)

To link to this article: <http://dx.doi.org/10.1080/14756366.2016.1247057>



© 2017 The Author(s). Published by Informa UK Limited, trading as Taylor & Francis Group



[View supplementary material](#)



Published online: 23 Jan 2017.



[Submit your article to this journal](#)



[View related articles](#)



[View Crossmark data](#)

RESEARCH ARTICLE

Exhaustive CoMFA and CoMSIA analyses around different chemical entities: a ligand-based study exploring the affinity and selectivity profiles of 5-HT_{1A} ligands

Sara Guariento^a, Silvia Franchini^b, Michele Tonelli^a, Paola Fossa^a, Claudia Sorbi^b, Elena Cichero^a and Livio Brasili^b

^aDepartment of Pharmacy, University of Genoa, Genoa, Italy; ^bDepartment of Life Sciences, University of Modena and Reggio Emilia, Modena, Italy

ABSTRACT

The 5-hydroxytryptamine (5-HT_{1A}) receptors represent an attractive target in drug discovery. In particular, 5-HT_{1A} agonists and partial agonists are deeply investigated for their potential role in the treatment of anxiety, depression, ischaemic brain disorder and more recently, of pain. On the other hand, 5-HT_{1A} antagonists have been revealed promising compounds in cognition disorders and, lately, in cancer. Thus, the discovery of 5HT_{1A} ligands is nowadays an appealing research activity in medicinal chemistry. In this work, Comparative Molecular Fields Analysis (CoMFA) and Comparative Molecular Similarity Index Analysis (CoMSIA) were applied on an in-house library of 5-HT_{1A} ligands bearing different chemical scaffolds in order to elucidate their affinity and selectivity for the target. Following this procedure, a number of structural modifications have been drawn for the development of much more effective 5-HT_{1A}R ligands.

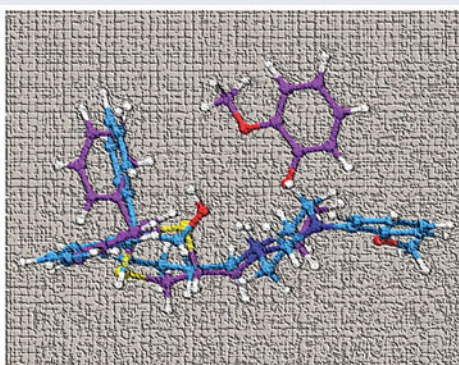
ARTICLE HISTORY

Received 10 July 2016
Revised 7 September 2016
Accepted 28 September 2016
Published online 4 November 2016

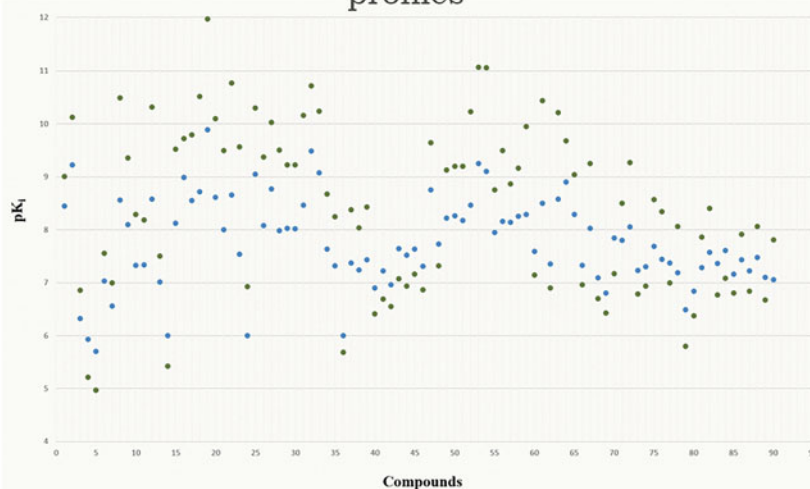
KEYWORDS

Adrenoreceptor; CoMFA;
CoMSIA; 5HT_{1A}-ligands;
3D-QSAR

Dioxolane-
Dithiolane-
Oxathiolane-
Tetrahydrofuran-
Cyclopentanol-
Cyclopentanone-
(spiro)anellated-
derivatives



3D-QSAR vs 5-HT_{1A} affinity and selectivity profiles



CONTACT Dr. Elena Cichero ✉ cichero@unige.it 📧 Department of Pharmacy, Section of Medicinal Chemistry, School of Medical and Pharmaceutical Sciences, University of Genoa, Viale Benedetto XV, 3, 16132 Genoa, Italy; Prof. Livio Brasili ✉ livio.brasili@unimore.it 📧 Department of Life Sciences, University of Modena and Reggio Emilia, Via Campi 103, 41125 Modena, Italy

📄 Supplemental data for this article can be accessed [here](#)

© 2017 The Author(s). Published by Informa UK Limited, trading as Taylor & Francis Group

This is an Open Access article distributed under the terms of the Creative Commons Attribution License (<http://creativecommons.org/licenses/by/4.0/>), which permits unrestricted use, distribution, and reproduction in any medium, provided the original work is properly cited.

Introduction

Serotonin (5-hydroxytryptamine, 5-HT) represents a key neurotransmitter playing a fundamental role especially at the central nervous system (CNS), being involved in numerous behavioural processes, such as anxiety, mood, aggression, addictive behaviours, as well as memory and learning processes, sleep, thermoregulation, appetite, emesis, thalamic blood pressure, nociception and migraine headaches¹. Up to now, at least 14 receptor subtypes (5-HT₁ to 5-HT₇) have been identified and therefore classified in terms of amino acid sequence and biological function. Among them, the 5-HT_{1A} receptor was the first one to be identified and pharmacologically investigated, relying on a number of ligands employed as pharmacological tools, such as BMY-7378 and WAY-100635^{2,3} (Figure 1). From a pharmaceutical point of view, the most interesting therapeutic potential of 5-HT_{1A} agonists and partial agonists revolves around the treatment of anxiety, depression, ischaemic brain disorder and, more recently, in pain^{3–5}. On the contrary antagonists of this receptor proved to be promising in cognition disorders, like Alzheimer's disease therapy⁶ and, lately, in cancer⁷.

On the other hand, due to the high pairwise similarity percentage between 5-HT_{1A}R and α_1 -adrenoreceptor (ADRs), a number of 5-HT_{1A} ligands proved to efficiently bind also to ADRs, at the expense of selectivity, as shown for instance in Figure 1 around the references BMY-7378 and WAY-100635. The α_1 adrenergic receptors (α_1 -ADRs) are deeply involved in the modulation of the activity of the sympathetic nervous system, becoming relevant druggable targets for many therapeutic agents. α_1 -ADRs are classified into at least three subtypes named α_{1A} , α_{1B} and α_{1D} . Antagonists of these receptors have been initially introduced for hypertension management, being later explored also for the treatment of benign prostatic hyperplasia (BPH)⁸.

During the last years, we focussed our attention on the development of new classes of potent 5-HT_{1A} receptor ligands, including 1,3-dioxolane-, 1,3-oxathiolane-, 1,3-dithiolane-, spiro-dioxolane-tetrahydrofuran-, cyclopentanone- and cyclopentanol-based derivatives, whose 5-HT_{1A} versus ADRs selectivity profiles were variable being in particular overall lower those towards the α_{1D} subtype^{9–15}. Here, with the aim of further exploring the key requirements to enhance the serotonergic affinity and selectivity over α_{1D} ADR, a three-dimensional quantitative structure–activity relationship (3D-QSAR) ligand-based computational protocol was applied to the aforementioned in-house library of compounds. In particular, we performed Comparative Molecular Fields Analysis (CoMFA) and a Comparative Molecular Similarity Index Analysis (CoMSIA), which represent useful tools to investigate the affinity as well as the selectivity profiles of compounds^{16–22}.

The role played by steric, electrostatic, H-bond acceptor and donor and hydrophobic features with respect to the 5-HT_{1A} affinity and selectivity trends observed within the library of ligands

suggested some structural modifications which could be useful for the development of new chemical scaffolds with an improved affinity and selectivity profile for 5-HT_{1A} receptor. The reliability of the final models was consistent with the effectiveness of an external series of 5-HT_{1A} ligands, giving a further validation of the 3D-QSAR studies here discussed. Moreover the results allowed us to derive robust statistical models to be used to predict the affinity of new analogues prior to synthesis and therefore to pave the way for the further design of more promising derivatives.

Methods

Dataset

In this work, the employed dataset included 81 compounds already synthesised by some of us (compounds **1–91**)^{10–15}. These molecules were divided into two groups according to the different linker between the five-membered ring and the terminal aromatic moiety of the scaffold, as shown in Tables 1 and 2. Group A (**1–42**; Table 1) included flexible open linker derivatives, while Group B (**43–91**; Table 2) contained all the piperazine ones. Tables 1 and 2 are also listed the 5HT_{1A} pK_i and the α_{1D} pK_i. Any details concerning the biological assays performed to evaluate the compounds affinity towards 5HT_{1A} receptors and ADRs have been reported in the previously cited works.

Any compound was built, parameterised (Gasteiger-Hückel method) and energy minimised within MOE using MMFF94 force field²³.

Notably, since all the analysed compounds displayed at least one chiral carbon atom, the selection of the most proper enantiomer was required for the further ligand-based studies. As far as we knew from our previous experimental studies on enantiomeric resolution of compound **1**, the stereoselectivity of the derivative was poor being (S)-**1** 5-HT_{1A} pK_i=8.42 and (R)-**1** 5-HT_{1A} pK_i=8.52²⁴.

For this reason, we considered to rely on these data and therefore to select for the *in silico* design (and alignment) those enantiomers along the whole dataset which proved to be also recommended by our docking results, as we previously detailed^{12,14,15}.

Briefly, within both Group A and B diphenyl-substituted dioxolane compounds were selected as *cR* enantiomers (as suggested by the enantiomeric resolution of **1**) as well as for the tetrahydrofurans and cyclopentanones, while the *cis* and *trans* mono-phenyl substituted ones followed the preferred *aS,cR* and *aR,cR* conformers. The *cis* and *trans* isomers of the cyclopentanol-based derivatives of Group A were recommended as *bR,cS* and *bR,cR* enantiomers. Those belonging to Group B were selected as *bS,cR* and *bR,cR* enantiomers. Lactam- and imide-based molecules were

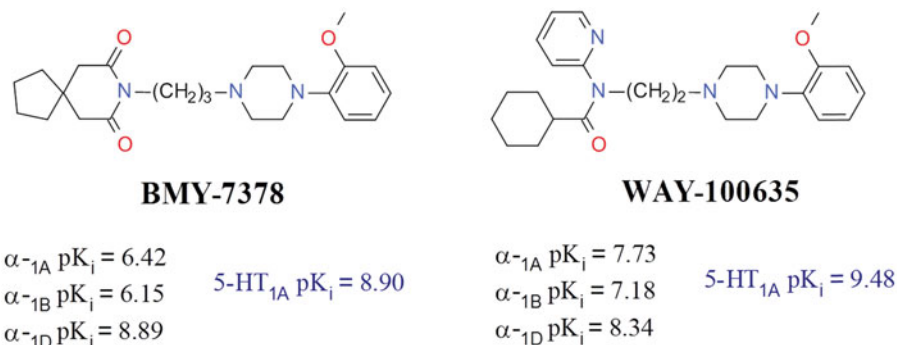
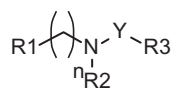
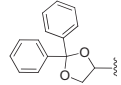
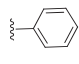
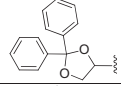
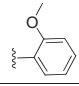
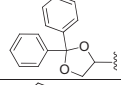
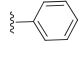
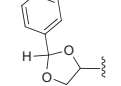
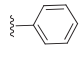
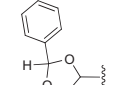
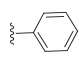
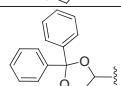
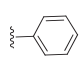
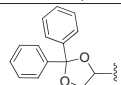
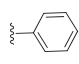
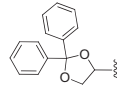
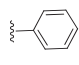
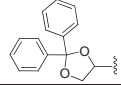
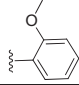
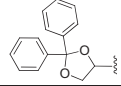
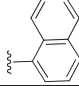
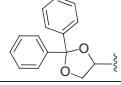
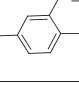
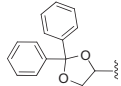
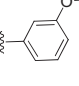
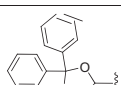
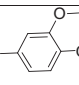
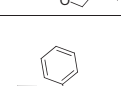
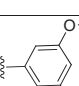
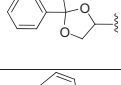
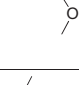
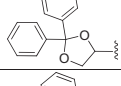
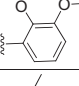


Figure 1. Chemical structure of the ligands BMY-7378, WAY-100635 and the related α_1 -ADR and 5-HT_{1A} affinity values.

Table 1. Chemical structures of compounds 1–42 (Group A).

Comp.	R ₁	n	R ₂	Y	R ₃	5-HT _{1A} pK _i	α-1D pK _i
1		1	H	-CH ₂ CH ₂ O-		8.45	8.37
2		1	H	-CH ₂ CH ₂ O-		9.22	8.65
3		1	CH ₃	-CH ₂ CH ₂ O-		6.32	6.06
4 cis		1	H	-CH ₂ CH ₂ O-		5.93	7.09
5 trans		1	H	-CH ₂ CH ₂ O-		5.70	6.94
6		1	H	-CH ₂ CH ₂ S-		7.03	6.87
7		1	H	-CH ₂ CH ₂ NH-		6.56	6.49
8		1	H	-CH ₂ CH ₂ CH ₂ -		8.56	6.28
9		1	H	-CH ₂ CH ₂ CH ₂ -		8.10	6.86
10		1	H	-CH ₂ CH ₂ O-		7.33	6.49
11		1	H	-CH ₂ CH ₂ O-		7.34	6.69
12		1	H	-CH ₂ CH ₂ O-		8.58	6.61
13		1	H	-CH ₂ CH ₂ O-		7.01	6.90
14		1	H	-CH ₂ CH ₂ O-		<6	6.77
15		1	H	-CH ₂ CH ₂ O-		8.12	6.64
16		1	H	-CH ₂ CH ₂ O-		8.99	8.68

(continued)

Table 1. Continued

Comp.	R ₁	n	R ₂	Y	R ₃	5-HT _{1A} pK _i	α-1D pK _i
17		1	H	CH ₂ CH ₂ O-		8.55	7.37
18		1	H	-CH ₂ CH ₂ CH ₂ -		8.72	6.66
19		1	H	-CH ₂ CH ₂ O-		9.89	7.50
20		1	H	CH ₂ CH ₂ O-		8.61	7.05
21		1	H	-CH ₂ CH ₂ CH ₂ -		8.00	6.36
22		1	H	-CH ₂ CH ₂ O-		8.66	6.10
23		1	H	-CH ₂ CH ₂ O-		7.54	< 5
24		1	H	-CH ₂ CH ₂ O-		<6	5.08
25		1	H	-CH ₂ CH ₂ O-		9.05	7.91
26		1	H	-CH ₂ CH ₂ O-		8.08	6.77
27		1	H	-CH ₂ CH ₂ O-		8.77	7.59
28		1	H	-CH ₂ CH ₂ O-		7.98	6.30
29 cis		1	H	-CH ₂ CH ₂ O-		8.03	6.88
30 trans		1	H	-CH ₂ CH ₂ O-		8.02	6.86
31		1	H	-CH ₂ CH ₂ O-		8.46	6.54
32 trans		1	H	-CH ₂ CH ₂ O-		9.49	8.42
33		1	H	-CH ₂ CH ₂ O-		9.08	8.09

(continued)

Table 1. Continued

Comp.	R ₁	n	R ₂	Y	R ₃	5-HT _{1A} pK _i	α _{1D} pK _i
34 E		1	H	-CH ₂ CH=CH-		7.63	6.68
35		1	H	-CH ₂ CH ₂ -		7.32	6.53
36		1	H	-CH ₂ -		<6	6.04
37		1	H	-CH ₂ CH ₂ CH ₂ CH ₂ -		7.37	6.46
38		2	H	-CH ₂ CH ₂ CH ₂ -		7.24	6.65
39		1	H	-CH ₂ CH ₂ O-		7.43	6.54
40		1	H	-CH ₂ CH ₂ O-		6.90	7.31
41		1	H	-CH ₂ CH ₂ O-		7.22	7.68
42		1	H	-CH ₂ CH ₂ O-		6.96	7.12

chosen as *aR,cS* isomers, while spiro-derivatives were preferred as *aR,cR*.

Consequently, in order to apply a common and homogeneous protocol, for all the dataset compounds we assigned the 5-HT_{1A} pK_i of the racemic mixture to the preferred enantiomers.

The followed alignment process considered the existing differences in conformation due to the various flexibility of Group A and B molecules. Initially, the most probable conformers of compounds **2** and **43** (taken as references for Group A and B, respectively) were superimposed using the rigid body alignment protocol implemented in MOE. Therefore, the flexible alignment approach of MOE was applied to guide a proper alignment of all the compounds of each group on the already aligned derivatives, used as rigid templates. Successively, the dataset was submitted to 3D-QSAR analyses, including CoMFA²⁵ and CoMSIA²⁶ studies, by Sybyl-X 1.0 software²⁷.

3D-QSAR analyses

CoMFA and CoMSIA approaches were performed to better understand especially how the steric and electrostatic parameters so as the hydrophobic, H-bond acceptor and H-bond donor descriptors could modulate the selectivity over α_{1D} ADR (Model I) and the affinity for 5-HT_{1A} receptor (Model II) of the whole dataset here proposed. Both the Models I and II were built considering the selectivity-based weighted 5-HT_{1A} pK_i (Model I) and the experimental 5-HT_{1A} pK_i (Model II) as the dependent variables while the

different specific CoMFA and CoMSIA descriptors were taken into account as independent ones.

In particular, for Model I, the ligand affinity towards the 5-HT_{1A} receptor has been re-calculated by taking into account the selectivity over α_{1D} ADR, following a procedure we recently applied around the development of selective PDE4B¹⁶ and PDE7 inhibitors²¹.

In this case, we considered the difference in pK_i between the 5-HT_{1A} and α_{1D} ADR and the related ratio, obtaining a selectivity-based weighted 5-HT_{1A} pK_i, according to Equations (1) and (2), which are described as follows. Equation (1) was applied for those compounds displaying higher or comparable α_{1D} ADR and 5-HT_{1A} pK_i while Equation (2) for the most selective 5-HT_{1A} ligands.

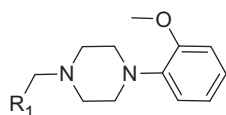
$$\text{Weighted 5-HT}_{1A} \text{ pK}_i = 5\text{-HT}_{1A} \text{ pK}_i \times \text{MR} + [(5\text{-HT}_{1A} \text{ pK}_i - \alpha_{1D} \text{ pK}_i) \times \text{MD}] \quad (1)$$

MR is the mean of the ratio between the 5-HT_{1A} and the α_{1D} pK_i values observed within all the molecules characterised by MR values ≤1.0 and MD the mean of the difference between the 5-HT_{1A} and the α_{1D} pK_i values of the same set of compounds.

$$\text{Weighted 5-HT}_{1A} \text{ pK}_i = 5\text{-HT}_{1A} \text{ pK}_i \times \text{MR} + [(5\text{-HT}_{1A} \text{ pK}_i - \alpha_{1D} \text{ pK}_i) \times \text{MD}'] \quad (2)$$

MR is the mean of the ratio between the 5-HT_{1A} and the α_{1D} pK_i values observed within all the molecules characterised by MR spanning from 1.0 to 1.2 and MD' the mean of the difference

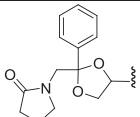
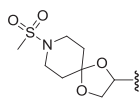
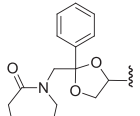
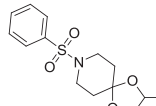
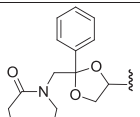
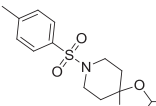
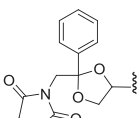
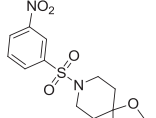
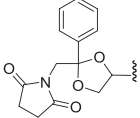
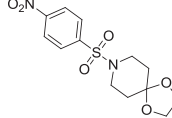
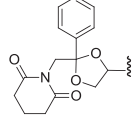
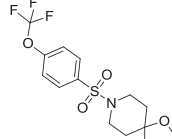
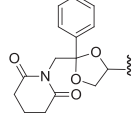
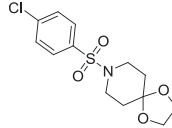
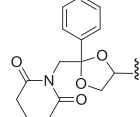
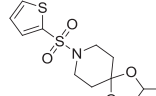
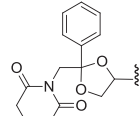
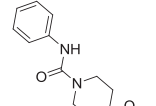
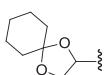
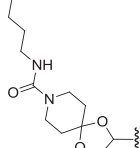
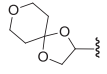
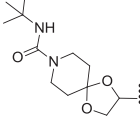
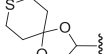
Table 2. Chemical structure of compounds 43–91 (Group B).



Comp.	R ₁	pK _i		Comp. p.	R ₁	pK _i	
		5-HT _{1A}	α-1D			5-HT _{1A}	α-1D
43		7.64	8.14	68		6.93	n.d.
44 cis		7.52	8.11	69		7.09	7.20
45 trans		7.63	7.86	70		6.80	6.89
46 cis		7.31	7.54	71		7.84	8.60
47 trans		8.75	8.16	72		7.80	7.43
48 cis		7.73	7.80	73		8.05	6.87
49 trans		8.22	7.55	74		7.23	7.45
50		8.26	7.52	75		7.30	7.29
51		8.18	7.33	76		7.69	7.02
52		8.46	6.43	77		7.44	6.71
53 cis		9.25	7.21	78		7.37	7.38
54 trans		9.10	6.82	79		7.19	6.48
55 trans		7.95	7.43	80		6.49	7.50

(continued)

Table 2. Continued

Comp.	R ₁	pK _i		Com p.	R ₁	pK _i	
		5-HT _{1A}	α-1D			5-HT _{1A}	α-1D
56 cis		8.16	6.79	81		6.84	7.18
57 trans		8.14	7.75	82		7.28	7.05
58 cis		8.25	7.57	83		7.57	6.96
59 cis		8.29	6.42	84		7.36	7.98
60 trans		7.59	7.78	85		7.61	8.02
61 cis		8.50	6.19	86		7.16	7.36
62 trans		7.35	7.57	87		7.43	7.37
63 cis		8.58	6.78	88		7.22	7.27
64 trans		8.90	8.51	89		7.48	7.26
65		8.29	7.88	90		7.10	7.29
66		7.33	7.33	91		7.06	6.53
67		8.03	6.84				

between the 5-HT_{1A} and the α_{1D} pK_i values of the whole dataset. For molecules displaying MR >1.2 this term is approximated to 1.0.

Following this procedure, the variation of the weighted pK_i values within the dataset concerns 5 log orders, being most of the selective compounds endowed with a weighted pK_i spanning from 8.00 up to 10.00. Conversely, the unselective (or reversed selective) molecules fall in the range of 5.00–8.00.

Notably, it is expected that such a weighted parameter could be much more predictive of the ligand selectivity profile over the α_{1D} ADR subtype observed within the chemical space disclosed around the whole dataset here investigated.

Training set and test set

Concerning Model I, the overall dataset was divided into a training set (68 compounds), for model generation, and in a test set (22 compounds), for model validation, being compound **68** excluded since it was not evaluated for α_{1D} ADR activity. For the development of Model II, 73 and 18 molecules were assigned to the training set and the test set, respectively.

For both the models, compounds were divided (in training and the test sets) manually in order to include a representative range of biological activities and structural variations of the starting dataset and including in the test set at least 25% of the number of training set molecules. Binding affinity values (pK_i) range of the compounds covered at least 4 log orders of magnitude.

CoMFA and CoMSIA models and statistical evaluation

CoMFA and CoMSIA methods are widely used 3D-QSAR techniques which allow to relate any variation of an experimental parameter (dependent variable) within a series of compounds with respect to specific descriptors (independent variables). In details, the steric and electrostatic fields and also the steric, electrostatic, hydrophobic, H-bond donor, H-bond acceptor ones were employed for CoMFA and CoMSIA analyses, respectively. Starting from a proper molecule alignment within a 3D cubic lattice (with a 2 Å grid spacing), the descriptor was calculated, using the standard Tripos force field method. Successively, the derived model goodness and reliability were evaluated using specific statistical tools, such as partial least square (PLS) analysis and cross-validation methods.

Finally, the predictive ability concerning those compounds belonging to the test set (r^2_{pred}) was also calculated, by means of the following equation:

$$r^2_{pred} = (SD - PRESS) / SD$$

being SD and PRESS the sum of the squared deviations between the biological activities of the test set molecules and the mean activity of the training set compounds, and the squared deviation between the observed and the predicted activities of the test set compounds, respectively.

Any further detail concerning the (standard) CoMFA and CoMSIA protocols and the related statistical and predictive evaluation we applied were previously reported in a number of our works^{28–30}.

Results

CoMFA and CoMSIA analyses here reported were used to explore, through quantitative methods, the main features responsible of the activity of an in-house library of 91 compounds as 5-HT_{1A}R ligands, and also of their related selectivity profile over α_{1D} ADR^{9–15}.

As shown in Figure 2, the whole dataset included molecules displaying a basic nitrogen, incorporated in a linear (in particular ethanolamine, cysteamine, ethylenediamine, methylamine, ethylamine, propylamine, butylamine, allylamine) or piperazine moiety, connecting a five-membered heterocycle or carbocycle (in particular dioxolane, 1,3-oxathiolane, 1,3-dithiolane, tetrahydrofurane, cyclopentanone, cyclopentanol and spiro-dioxolane) bringing at least a phenyl ring or a spiro appendage. The members of the library were divided into two groups, A and B, depending on whether the basic nitrogen is part of the flexible chain or is incorporated into the piperazine ring (Tables 1 and 2, respectively).

Energy minimisation and alignment of the dataset highlighted a relevant difference in the preferred conformation between Group A and B. In particular, for the molecules of Group A, a U-shaped conformation was the energetically favoured one, while a much more linear disposition was found for Group B compounds (Supplemental data S1). On the overall alignment, we performed two series of 3D-QSAR analyses.

In detail, the first CoMFA and CoMSIA study (Model I) was performed around the selectivity profile over α_{1D} using a weighted pK_i (as described in the experimental section) while the second one analysed 5HT_{1A} potency trend using the ligands experimental 5-HT_{1A} affinity values (Model II).

3D-QSAR analyses

Concerning Model I CoMFA and CoMSIA analyses were performed by dividing compounds **1–91** excluding **68** into a training set for

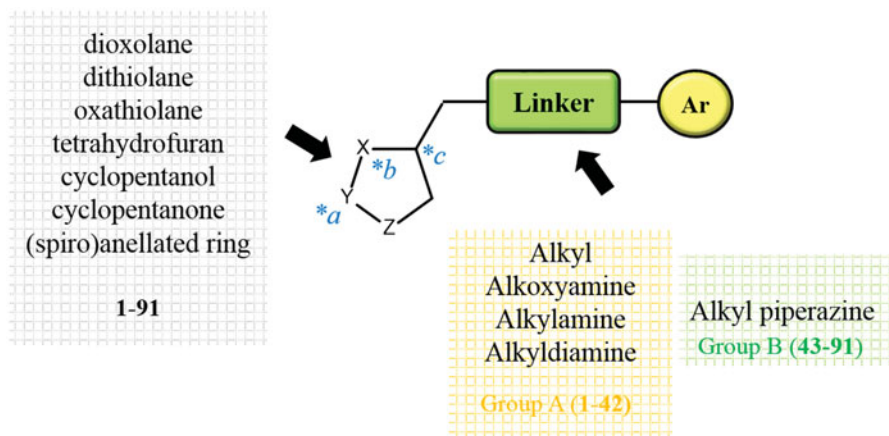


Figure 2. Schematic representation of the library members.

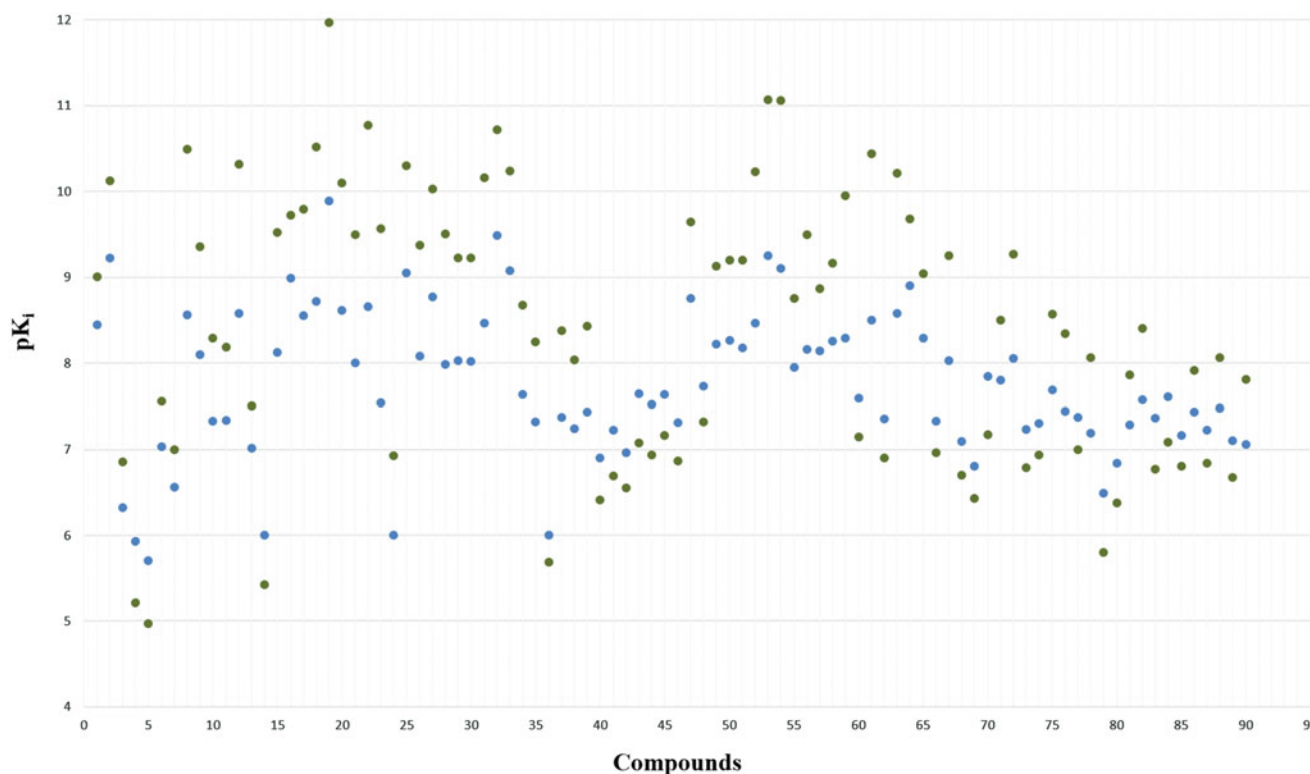


Figure 3. Distribution of the experimental-based weighted affinity and of the experimental ones of the dataset compounds.

model generation and into a test set for model validation (see Methods section). A graphical distribution of the selectivity (green dots) and affinity profile (blue dots) of the dataset compounds is shown in Figure 3.

Model II CoMFA and CoMSIA studies were calculated including sixty-eight derivatives into the training set and choosing the other molecules for the test set.

All statistical parameters supporting the two series of 3D-QSAR analyses (Models I and II) are reported in Table 3 and detailed as follows.

The final Model I CoMFA was generated by employing non-cross-validated PLS analysis with the optimum number of components (ONC = 7) to give a non-cross validated r^2 (r^2_{ncv}) = 0.94, a test set r^2 (r^2_{pred}) = 0.80, standard error of estimate (SEE) = 0.278, steric contribution = 0.678 and electrostatic contribution = 0.322.

The related CoMSIA analysis was derived using a statistical PLS analysis leading to the following results: ONC = 6, a non-cross validated r^2 (r^2_{ncv}) = 0.93, a test set r^2 (r^2_{pred}) = 0.79, SEE = 0.312, steric contribution = 0.173, electrostatic contribution = 0.139, hydrophobic contribution = 0.358, H-bond acceptor = 0.213 and H-bond donor = 0.117.

An overall overview of the predictive ability of Model I study can be obtained from graphical distributions of the predicted weighted pK_i values of the training set (blue dots) and test compounds (red dots), as shown in Figure 4. The corresponding experimental-based and predicted pK_i values are reported as Supplemental data S2 and S3.

The selected CoMFA Model II was generated by employing non-cross-validated PLS analysis with the ONC = 6 to give a non-cross validated r^2 (r^2_{ncv}) = .92, a test set r^2 (r^2_{pred}) = .78, SEE = 0.294, steric contribution = 0.644 and electrostatic contribution = 0.356. The CoMSIA Model II was obtained with the following statistical results: ONC = 6, a non-cross validated r^2 (r^2_{ncv}) = .91, a test set r^2 (r^2_{pred}) = .77, SEE = 0.280, steric contribution = 0.175,

Table 3. Summary of CoMFA and CoMSIA analyses calculated as Models I and II.

	Model I		Model II	
	CoMFA	CoMSIA	CoMFA	CoMSIA
No. compounds	68	68	73	73
Optimal number of components (ONC)	7	6	6	6
Leave one out r^2 (r^2_{loo})	0.60	0.58	0.62	0.55
Cross-validated r^2 (r^2_{cv})	0.75	0.74	0.73	0.71
Std. error of estimate (SEE)	0.278	0.312	0.294	0.280
Non cross-validated r^2 (r^2_{ncv})	0.94	0.93	0.92	0.91
F-value	101.014	65.725	87.006	64.876
Steric contribution	0.678	0.173	0.644	0.175
Electrostatic contribution	0.322	0.139	0.356	0.155
H-bond acceptor contribution	–	0.213	–	0.214
H-bond donor contribution	–	0.117	–	0.104
Hydrophobicity contribution	–	0.358	–	0.352
Bootstrap r^2 (r^2_{boot})	0.97	0.95	0.94	0.93
Standard error of estimate r^2_{boot} (SEE r^2_{boot})	0.268	0.271	0.250	0.280
Test set r^2 (r^2_{pred})	0.80	0.79	0.78	0.77

electrostatic contribution = 0.155, hydrophobic contribution = 0.352, H-bond acceptor = 0.214 and H-bond donor = 0.104.

The derived distributions of the predicted pK_i values of the training set and test compounds are depicted in Figure 5 while the specific experimental and predicted affinity values are reported as Supplemental data S4 and S5.

Discussion

CoMFA and CoMSIA contour maps

Notably, for both the Models I and II, the CoMFA steric map descriptors underlines through green polyhedra those areas which prove to be favourable in terms of steric hindered substitutions, while yellow maps highlight regions where bulky decorations impaired the 5-HT_{1A} selectivity (for Model I) or affinity (for Model II) profile. The CoMFA electrostatic descriptors are shown as blue

Model I CoMFA and CoMSIA analyses

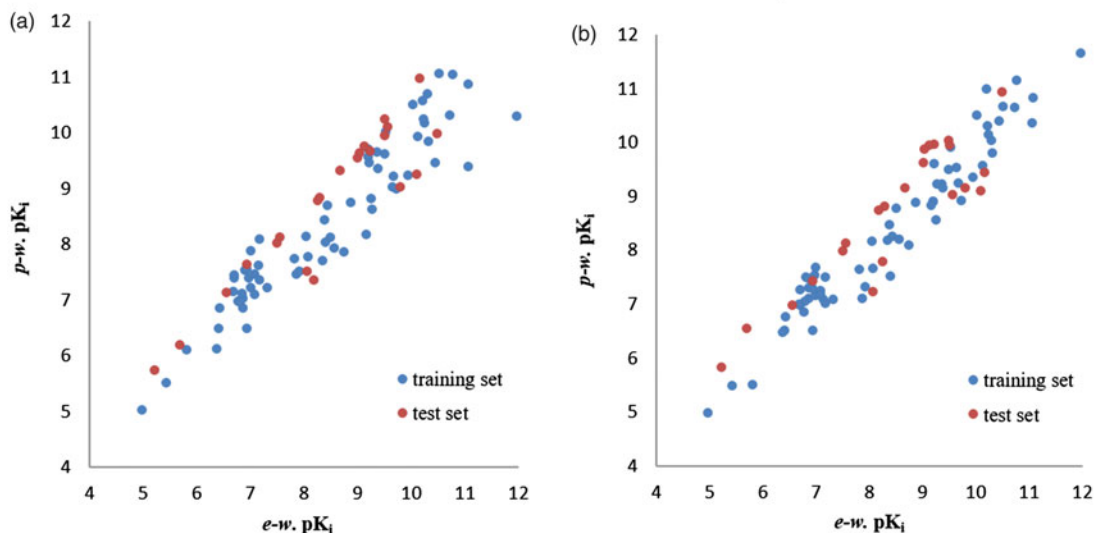


Figure 4. Distribution of the predicted weighted pK_i values ($p-w. pK_i$) with respect to the experimental-based pK_i ($e-w. pK_i$) of the training set compounds and of the test set compounds according to Model I CoMFA (a) and CoMSIA (b) analyses.

Model II CoMFA and CoMSIA analyses

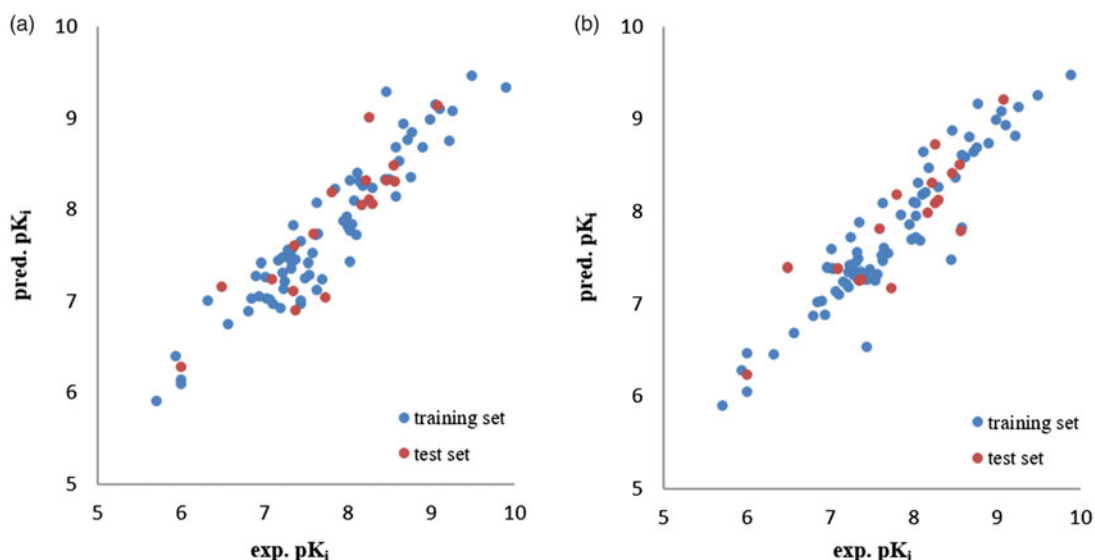


Figure 5. Distribution of the predicted pK_i values of training set compounds and of the test set compounds with respect to the experimental data according to Model II CoMFA (a) and CoMSIA (b) analyses.

areas around regions which tolerate electropositive groups, while red polyhedra occupy any area where electronegative groups enhance the selectivity (or affinity) towards the target.

Concerning CoMSIA analyses, the yellow and white hydrophobic contours suggest the insertion of lipophilic and polar groups, respectively.

Finally, the introduction of H-bond acceptor and H-bond donor moieties is encouraged or discouraged by magenta and cyan and green (or red for Model II) and purple polyhedral, respectively.

Model I (5HT_{1A} ligand selectivity over α_{1D} ADR)

Based on an overall analysis of the CoMFA steric map, it could be observed that those compounds belonging to Group A much

more properly fit the contour map, rather than the Group B analogues (see Figure 6(a) and (b)). Indeed, the presence of a flexible linker allows to arrange R1 of Group A compounds in proximity of a large favoured green area, while the piperazine ring of Group B moves this substituent to a quite switched positioning.

As a consequence, for Group A the diphenyl-substituted derivatives are adequately projected towards the aforementioned large green area, and also close to a second small one, while the spiro-derivatives **40–42** fall in a disfavoured yellow area (Figure 6(a)).

Accordingly, most of the diphenyl-substituted compounds **1–38** are characterised by an acceptable selectivity profile, while spiro-derivatives led sometimes to a reversed potency trend [see **40** (5-HT_{1A} pK_i = 6.90, α_{1D} pK_i = 7.31) **41** (5-HT_{1A} pK_i = 7.22, α_{1D} pK_i = 7.68), **42** (5-HT_{1A} pK_i = 6.96, α_{1D} pK_i = 7.12)]. Nevertheless, spiro-compounds could be optimised in selectivity by proper further

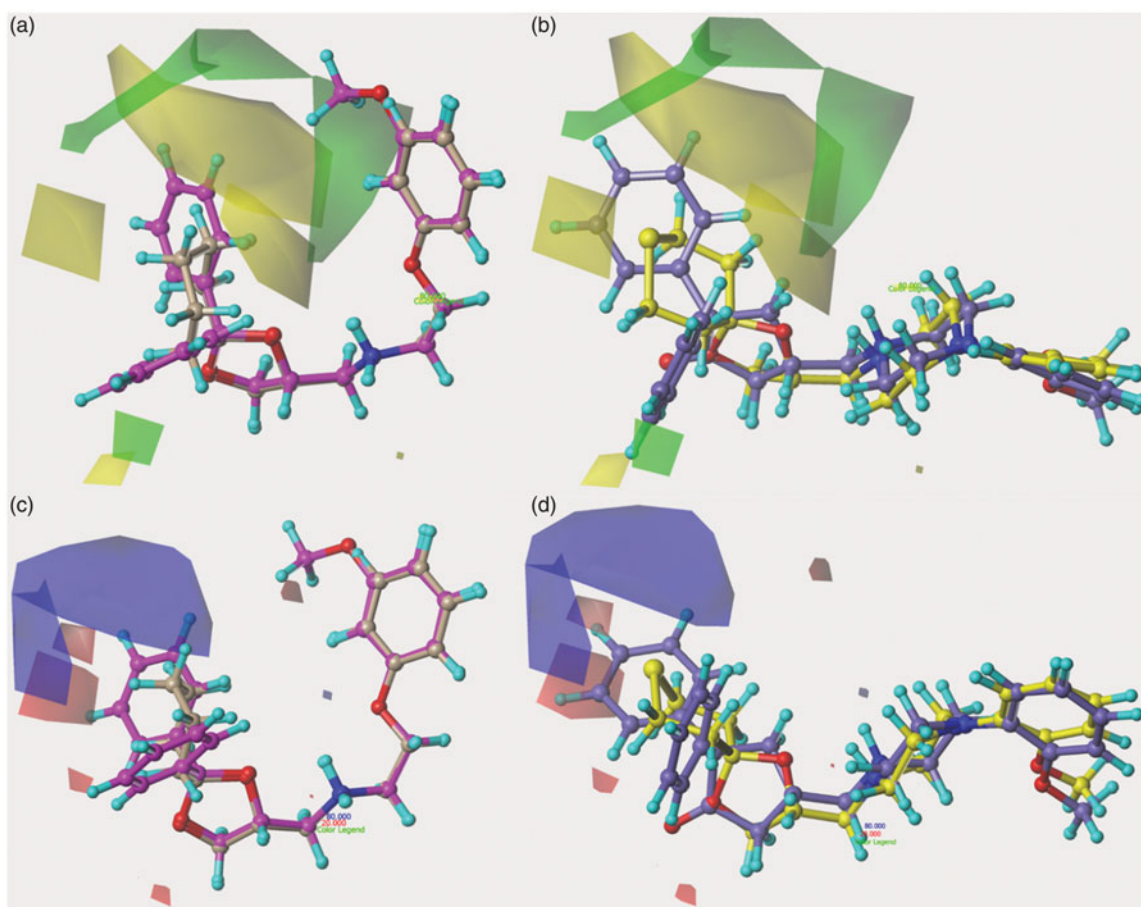


Figure 6. Contour map of Model I CoMFA steric regions are shown around the compounds **12** and **39** (a) and **52**, **67** (b) while those of the electrostatic map are shown in (c) and (d).

decoration, such as those described within Group B (see compounds **68–78**) including bulky H-bond acceptor moieties, gaining new contacts with the green map.

Furthermore, the presence of a proper linker Y, as a propyl chain, optimises the overall flexibility of the molecule and allow the terminal phenyl ring and also R1 to better overlap the favoured steric contours. Consequently, compounds **8** (Y = $-\text{CH}_2\text{CH}_2\text{CH}_2-$; 5-HT_{1A} pK_i = 8.56, α_{1D} pK_i = 6.28), **9** (Y = $-\text{CH}_2\text{CH}_2\text{CH}_2-$; 5-HT_{1A} pK_i = 8.10, α_{1D} pK_i = 6.86) and **18** (Y = $-\text{CH}_2\text{CH}_2\text{CH}_2-$; 5-HT_{1A} pK_i = 8.72, α_{1D} pK_i = 6.66) result to be much more selective than the analogues **1** (Y = $-\text{CH}_2\text{CH}_2\text{O}-$; 5-HT_{1A} pK_i = 8.45, α_{1D} pK_i = 8.37), **2** (Y = $-\text{CH}_2\text{CH}_2\text{O}-$; 5-HT_{1A} pK_i = 9.22, α_{1D} pK_i = 8.65) and **17** (Y = $-\text{CH}_2\text{CH}_2\text{O}-$; 5-HT_{1A} pK_i = 8.55, α_{1D} pK_i = 7.37), respectively.

Interestingly, the ligand selectivity does not take advantage from the introduction of any decoration onto the terminal phenyl ring *ortho* positions. Indeed, moving from **8** (R3 = phenyl; 5-HT_{1A} pK_i = 8.56, α_{1D} pK_i = 6.28) and **20** (R3 = phenyl; 5-HT_{1A} pK_i = 8.61, α_{1D} pK_i = 7.05) to the 2-methoxy-substituted congeners **9** (R3 = 2-methoxyphenyl; 5-HT_{1A} pK_i = 8.10, α_{1D} pK_i = 6.86) and **19** (R3 = 2-methoxyphenyl; 5-HT_{1A} pK_i = 9.89, α_{1D} pK_i = 7.50), the ligand affinity trend reverses or increases towards both the receptors. This information is also supported by the biological results obtained for **26** (R3 = 2-methylphenyl; 5-HT_{1A} pK_i = 8.08, α_{1D} pK_i = 6.77), **25** (R3 = 2-ethoxyphenyl; 5-HT_{1A} pK_i = 9.05, α_{1D} pK_i = 7.91) and **27** (R3 = 2-isopropoxyphenyl; 5-HT_{1A} pK_i = 8.77, α_{1D} pK_i = 7.59).

Concerning the Group B compounds, the piperazine ring constrains the R1 substituent to be oriented towards a disfavoured

yellow area, leading most of the ligands far from the green one (Figure 6(b)). In particular, the spiro-substitution is the one that much more deeply impairs the selectivity within the group, as exemplified by **75–77** (5-HT_{1A} pK_i = 7.30–7.44, α_{1D} pK_i = 6.71–7.29)], with a poor selectivity profile for 5HT1-R over ADR- α_{1D} , whilst sometimes it results also reversed [see **69–71** (5-HT_{1A} pK_i = 6.80–7.84, α_{1D} pK_i = 6.89–8.60) and **84–86** (5-HT_{1A} pK_i = 7.16–7.61, α_{1D} pK_i = 7.37–8.02)].

Then, only the (potentially small) mono-substituted derivatives are those that appear fitting a green polyhedron. On the other hand, it should be noticed that the choice of introducing a lactam or imide moiety linked to the R1 five-membered ring could provide for a better overall flexibility. In particular, the related *cis* isomers, rather than the *trans* ones, achieve a conformation to efficiently contact the steric map. The reliability of this information can be verified comparing the selectivity profile of the *cis* conformers **56**, **58**, **59**, **61**, **63** (5-HT_{1A} pK_i = 8.16–8.58, α_{1D} pK_i = 6.19–7.57) with those of *trans* ones **55**, **57**, **60**, **62**, **64** (5-HT_{1A} pK_i = 7.35–8.90, α_{1D} pK_i = 7.43–8.51).

As shown in Figure 6(c) and (d), the electrostatic contour map reveals favoured region with the introduction of electro-negative groups (red polyhedral) in the area surrounding the spiro-derivatives and the diphenyl-substituted ones of Group A, also suggesting the presence of electropositive portions for bulkier groups in R1 (blue area). Interestingly, these results allow to point out the introduction of electro-withdrawing groups onto the spiro-derivatives or the development of

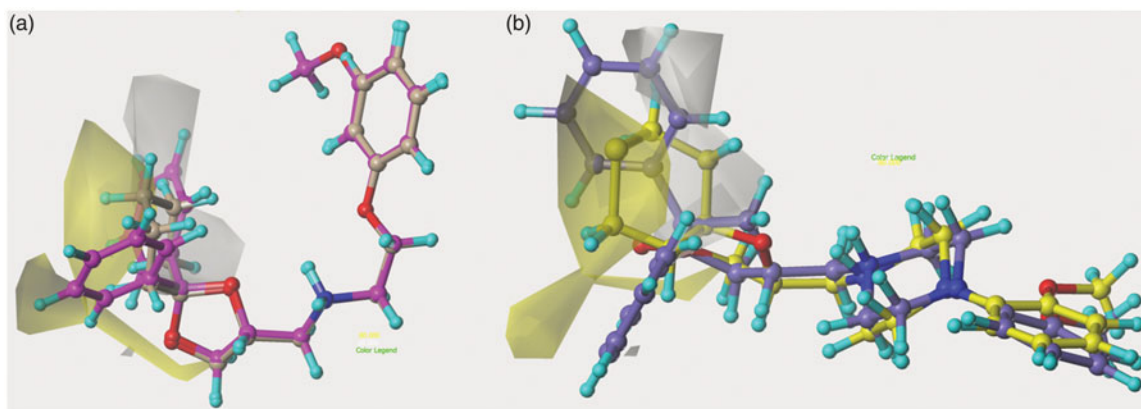


Figure 7. Model I CoMSIA hydrophobic favoured and disfavoured (white area) regions are shown around **12** and **39** (a) and **52**, **67** (b). The compounds are displayed in ball and stick mode.

analogues bearing lactam or imide moieties, as displayed within the Group B series.

On the other hand, a small blue area placed around oxygen atom of the linker Y in compounds **12** and **39** (Figure 6(c)) strongly confirms the beneficial role played by the propyl chain at this position (rather than the ethoxy one).

A comparable electrostatic preferences profile can be described for compounds belonging to Group B (see Figure 6(d)). Notably these results are in good agreement with the privileged role played by a lactam or imide moiety at the R1 five-membered ring, as revealed by the steric map.

The steric and electrostatic maps obtained from CoMSIA analysis were in good agreement with those derived from the previous CoMFA study.

Hydrophobic moieties are beneficial (yellow map) around the oxygen atom of tetrahydrofuran and near the corresponding heteroatom of the dioxolane, dithiolane and oxathionale derivatives, while one disfavoured region (white map) falls around the cyclopentanone or cyclopentanol functional moiety (Figure 7(a)). Consequently, any kind of these five-membered rings appears to have the proper polarity balance to encourage 5HT_{1A} selectivity of action.

Mono-substituted or diphenyl-substituted compounds of Group B better surround the hydrophobic yellow map, than the spiro-derivatives, which partially overlap the disfavoured white region (Figure 7(b)). This contour map proves to be reached properly by those compounds endowed with a flexible lactam or imide moieties, being the *cis* isomers the most favoured (see also the information coming from the steric map).

Magenta areas, favourable for H-bond acceptor moieties, are located in proximity of the two phenyl rings of the disubstituted derivatives of Groups A and B, being also highly overlapped by any lactam and imide moieties in R1, and are placed also in proximity of the spiro-derivatives of Group B (Supplemental data S6). Finally, H-donor favoured regions (cyan polyhedral) are fulfilled by the secondary amine nitrogen atom of the linker displayed within Group A, but not by the piperazine tertiary one (Supplemental data S7). Thus, the flexible linker is confirmed as the better choice to ameliorate the selectivity issue.

Model II (5HT_{1A} ligand affinity)

Since the first aim in the development of new 5HT_{1A} ligands is the design of compounds with an improved affinity profile, the description of Model II results was organised in four sections,

based on the various substitutions displayed by the molecules of interest: (i) part 1, including all the substitutions on the quaternary carbon atom of the five-membered ring; (ii) part 2, consisting of the five-membered ring (R1); (iii) part 3, formed by the linker Y; (iv) part 4, represented by the terminal aromatic ring (R3).

The derived Model II CoMFA and CoMSIA maps were reported in Charts 1 and 2, respectively. Only the CoMSIA hydrophobic, H-bond acceptor and H-bond donor descriptors were reported, since the steric and the electrostatic ones were highly similar to those shown for the related CoMFA study. In any case, the contour areas were depicted around compounds **19**, **39** and **53 cis**, **67** to represent Group A and B ligands, respectively.

Part 1

A favourable steric and hydrophobic polyhedra is detected in the centre of the area occupied by Part1 of the scaffold, which proved to be differently fitted by Group A and B derivatives because of the different conformer positioning of the flexible or the rigid linkers, respectively.

Thus, the affinity profile of mono-substituted, di-substituted and spiro-substituted compounds follows a different trend within the two groups. Indeed, within Group A, the mono-phenyl substitution is the most detrimental with respect to the di-phenyl and spiro-analogues, poorly satisfying the aforementioned contour maps. In addition, the insertion of a spiro or (spiro)anellated cycle results to be tolerated, being these compounds able to occupy partially the favoured steric areas and fully the hydrophobic map. Nevertheless, the (spiro)anellated **40–42** ($pK_i = 6.90–7.22$) display a lower 5HT_{1A} affinity profile, if compared with the di-substituted derivatives. Indeed, the di-substituted derivatives of Group A successfully overlap the aforementioned steric and hydrophobic regions, as confirmed by the adequate affinity profile of most of them (see **25–33**; $pK_i = 7.98–9.49$), pointing out this kind of substitution as the most effective within Group A. In particular, this conclusion can be confirmed especially comparing compound **1** ($pK_i = 8.45$) to **42** ($pK_i = 6.96$).

Finally, a consistent H-bond acceptor favourable area surrounds the part 1 of all these derivatives, suggesting a beneficial role potentially due to the introduction of proper H-bonding functions at this molecule portion.

Concerning Group B, the rigid linker constrains the ligand conformation to be arranged in a different and overall more effective positioning, which allows the part 1 of the molecule to better contact the contour maps. Thus, the di-substituted compounds

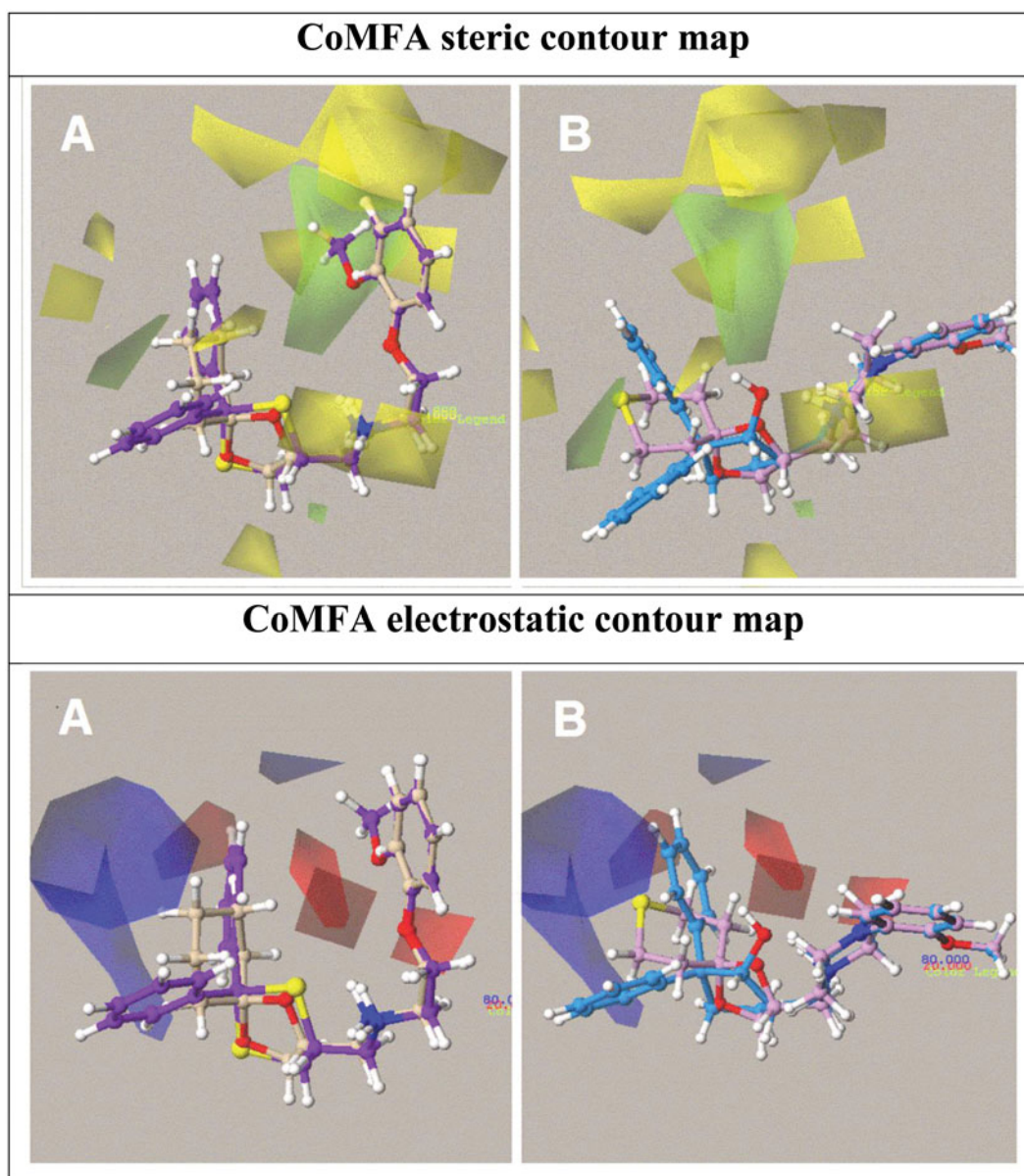


Chart 1. Contour maps of Model II CoMFA model steric and electrostatic regions are shown for Group A 19, 39 and Group B 53 *cis*, 67.

maintain an adequate ability to fit the CoMFA steric map, as previously discussed within the Group A analogues. In addition, also the mono-substituted- and the spiro-derivatives of Group B are much more properly oriented towards favoured steric and hydrophobic areas, as confirmed by the high affinity values of compounds **44–49** ($pK_i=7.31\text{--}8.75$) and **67** ($pK_i=8.03$).

Nonetheless, only small decorations on the spirocycle part 1 are tolerated, as shown by **71–91** ($pK_i=6.49\text{--}7.84$), which have lower $5HT_{1A}$ affinity than **67** ($pK_i=8.03$).

In addition, for the mono-substituted analogues, a privileged trend involving the *trans* isomers rather than the *cis* ones is highlighted [compare **48 cis** ($pK_i=7.73$) with **49 trans** ($pK_i=8.22$)].

Regarding the di-substituted compounds, CoMFA maps promoted the insertion of a hydrophobic and electronegative decoration in part 1 in the case of *trans* conformers, while electropositive and polar moieties are recommended for the *cis* ones. Accordingly, for the imide and lactam derivatives of the dataset the *cis* isomer was preferred rather than the *trans* one,

even if both showing good pK_i value [e.g. compare compounds **55 trans** ($pK_i=7.95$), **57 trans** ($pK_i=8.14$), **60 trans** ($pK_i=7.59$), **62 trans** ($pK_i=7.35$), with the related isomers **56 cis** ($pK_i=8.16$), **58 cis** ($pK_i=8.25$), **59 cis** ($pK_i=8.29$), **61 cis** ($pK_i=8.50$)]. In addition, an overall positive role played by the imide and lactam moieties is confirmed by an extended H-bond acceptor favoured area (magenta polyhedral) involving part 1.

Part 2

As regard the five-membered ring of the scaffold, 3D-QSAR analyses identify several defined features related to $5HT_{1A}$ binding affinity. For both the Groups A and B, CoMFA maps promote the introduction of substituent onto the atom connecting part 1 and part 3, in particular bearing electronegative groups, while the CoMSIA contours discourages any putative H-bond acceptor moiety around the whole five-membered ring. Interestingly, these information prove to be consistent with the higher affinity trend

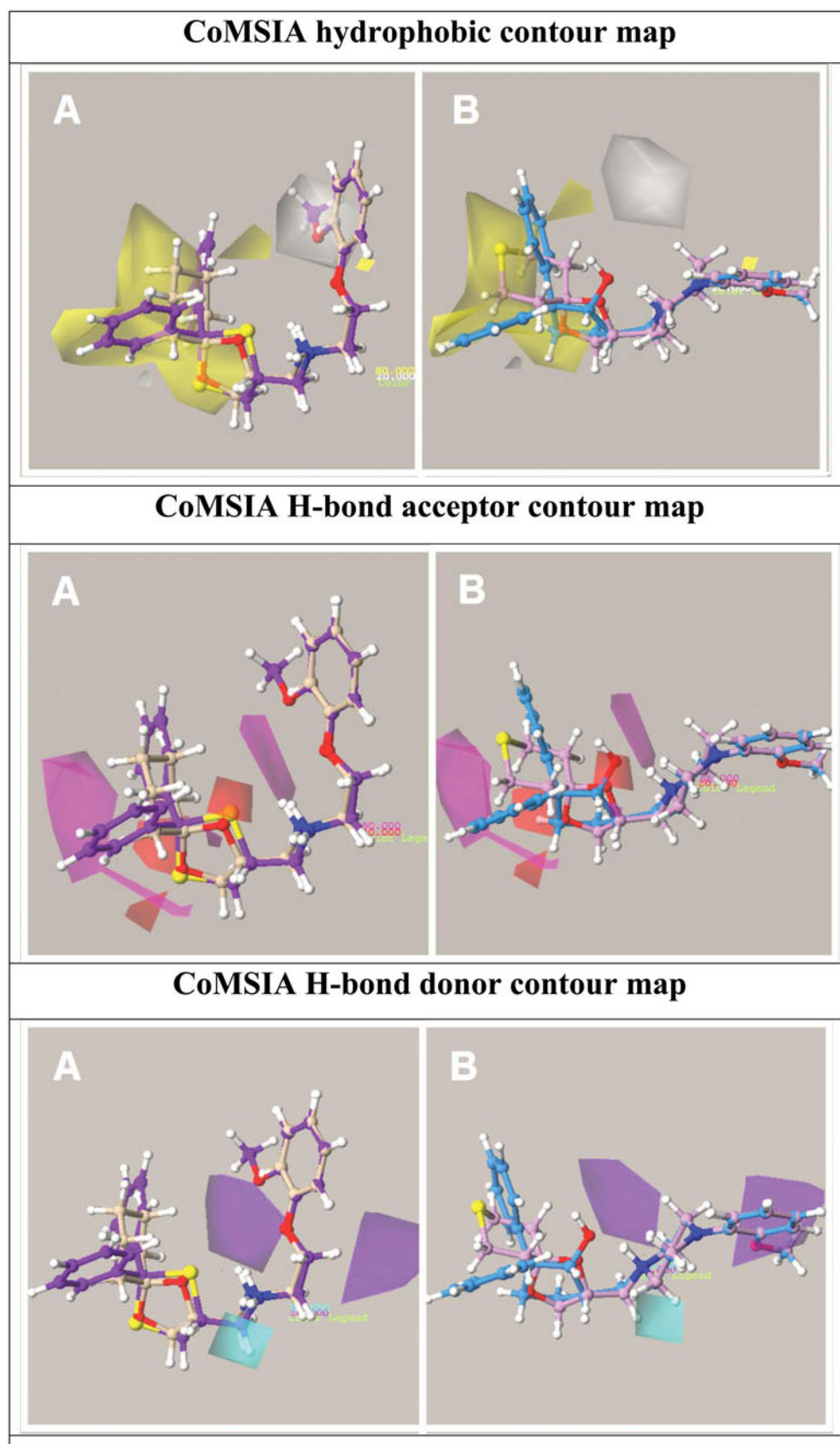


Chart 2. Contour maps of Model II CoMSIA model hydrophobic, H-bond acceptor and H-bond donor descriptors are shown. Compounds 19, 39 and 53 cis, 67 are depicted.

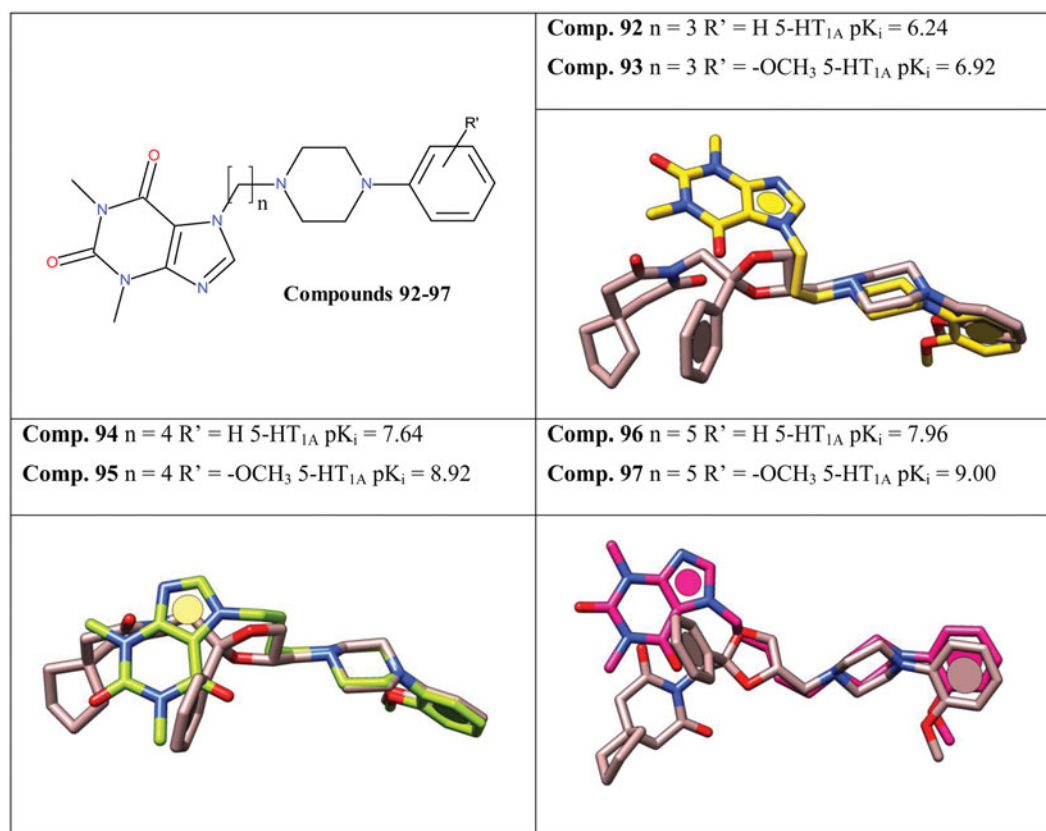


Chart 3. Superimpositions of the in-house derivative **63 cis** and the external set compounds **93**, **95** and **97** are depicted. The chemical structure and the 5-HT_{1A} affinity values for **92–97** are also shown.

observed within the cyclopentyloxy derivatives rather than that about the cyclopentanone ones

Notably, the five-membered ring of Group A derivatives highly fit the CoMSIA hydrophobic map, while the Group B counterparts are arranged in a slightly different conformation due to the rigid piperazine linker, preventing to fully overlap the aforementioned contour.

Based on an overall perspective of these results, the dithiolane ring appears to be the most adequate one for Group A, fully satisfying the aforementioned maps, as confirmed by higher affinity values of **19** ($pK_i = 9.89$) and **20** ($pK_i = 8.61$) if compared with **12** ($pK_i = 8.58$) and **1** ($pK_i = 8.45$), respectively. Concerning Group B, the replacement of the dioxolane core with the oxathiolane or dithiolane ones is anyway allowed, [see the higher affinity values of **50** ($pK_i = 8.26$) and **51** ($pK_i = 8.18$) with respect to **43** ($pK_i = 7.64$)].

Finally, the cyclopentanole ring exhibits a balanced lipophilicity profile and, particularly for Group B, results to properly satisfy the suggested CoMFA steric and electrostatic requirements, as verified by the effective cyclopentanole-based derivatives **53 cis** ($pK_i = 9.25$) and **54 trans** ($pK_i = 9.10$).

Part 3

The most relevant result of the 3D QSAR analysis about this part of the scaffold is the most positive steric effect of the open linker rather than the piperazine on 5HT_{1A} affinity. Bulky substitution at the linker level as well as the presence of an additional substitution on the secondary amine seems to be poorly and not allowed by the contours, as confirmed by the different affinity

profiles of compounds **1** ($pK_i = 8.45$) and **43** ($pK_i = 7.64$). In particular, the propylamine linker is tolerated, while longer or shorter carbon chains are embedded in an electronegative region at different levels, lowering the compound affinity for the target [see **35** ($Y = -CH_2CH_2-$; $pK_i = 7.32$), **36** ($Y = -CH_2-$; $pK_i < 6$) and **37** ($Y = -CH_2CH_2-CH_2CH_2-$; $pK_i = 7.37$)]. Finally, the encouraging effect of the secondary amine rather than the tertiary one is described by the presence of a close favoured H-donor contour that matches one of the two hydrogen of the amine linker of Group A derivatives.

Part 4

All the fields considered by CoMFA and CoMSIA studies reveal a positive role played by the 2-methoxyphenyl ring around the Group A derivatives. More in details, an electronegative contour (red polyhedral) close to one of the two *ortho* positions of the phenyl ring in R3 denotes the alkoxy decoration as a suitable choice to improve the affinity for the 5HT_{1A} receptor. This conclusion is also underlined by the presence of polar, unfavourable H-bond donor and favourable H-bond acceptor polyhedra in proximity of part 4.

On the other hand, a favourable steric polyhedron, surrounded by unfavourable contours, suggested that the insertion of bulkier substitutions than the methoxy one could impair the ligand affinity, making the methoxy group the most effective alkoxy moiety to be exploited.

This result may be verified by the decreasing affinity trend moving from compounds **2** (R3 = 2-methoxyphenyl; $pK_i = 9.22$), **25**

(R3 = 2-ethoxyphenyl; $pK_i = 9.05$) and **27** (R3 = 2-isopropoxyphenyl; $pK_i = 8.77$) to the biaryl analogue **22** ($pK_i = 8.66$).

Notably, the introduction of further groups in *meta* and *para* positions of the R3 phenyl ring was discouraged by the steric field. In particular, any structural modification including fused ring systems such as naphthyl moieties, or *meta* and/or *para* (di)substituted derivatives led to less active compounds.

For Group B compounds, less information were available since no example of compound with an un-substituted phenyl ring was collected by our "in-house" library of molecules.

Taking into account an overall perspective of Model I and II studies, the selection of an open linker rather than the piperazine seems to be the most effective for both affinity and selectivity, while piperazine derivatives could be further optimised through the introduction of a longer chain (than the methylene) connecting with the terminal phenyl ring.

In details, the selectivity issue seems to be related to an adequate flexibility profile of the molecule.

Thus, the design of novel ligands bearing a flexible linker combined with a diphenyl substitution or a proper branched decoration enriched with polar moieties such as the lactam and imide moieties onto the five-membered ring may derive new more selective compounds. Spiro-derivatives may be optimised by linking them to linear or to cyclic amine spacers and selecting additional polar functions as decoration for the spiro-group or longer linker including the basic core.

Notably, selectivity does not take advantage from the introduction of decorations onto the terminal phenyl ring, conversely to the results obtained around the 5-HT_{1A} affinity profile. In addition, while the presence of cyclopentanone and of dithiolane as five-membered rings is overall encouraged by Model II, only the dithiolane one (or generally a hydrophobic group) is the most recommended for selectivity (Model I).

It should be observed that the derived data are in harmony with the affinity and selectivity of reference compounds BMY-7378 and WAY-100635, which exhibit longer aliphatic chains connected to the piperazine ring in tandem with a 2-methoxy substitution onto the terminal phenyl ring. In particular, our observations about the decorations on the terminal phenyl ring are consistent with the high affinity but poor selectivity of the two.

Finally, in order to gain a qualitative validation of the results here discussed, we also evaluated the ability of Model II contour maps to rationalise the effectiveness of an external series of novel (pyperazinyl)alkyl-based 5-HT_{1A} ligands³¹. In particular, these compounds included a 1,3-dimethyl-purine-2,6-dione heterocycle as bio-isostere of R1 substituent of the in-house compounds included in Group B.

As shown in [Chart 3](#), structural similarity-based alignments of compounds **92–97** onto compound **63 cis** reveal that only a few number of these compounds are able to satisfy the requirements pointed out by Model II. Indeed, **93** only partially mimic through the purine-2,6-dione cycle the role played by the disubstituted dioxolane ring of **63 cis**, therefore displaying a lower pK_i value. Similarly, the related analogue **92**, unsubstituted onto the terminal phenyl moiety, proved to be poorly active as 5-HT_{1A} ligand lacking of proper contacts with the Model II steric map. Conversely, those derivatives exhibiting a butyl (**94**, **95**) or a pentyl (**96**, **97**) chain between the purine-2,6-dione and the piperazine spacer are able to fulfil the specific features highlighted by the Model II CoMFA steric and CoMSIA hydrophobic maps. Indeed, the aliphatic linker simulate the dioxolane of **63 cis** (and also the much more hydrophobic dithiolane ring we previously suggested), while the purine-based group is highly able to

reproduce the decoration enriched with polar moieties recommended in R1 by 3D-QSAR studies.

Conclusions

The computational studies here presented highlight and discuss the role played by the steric, electrostatic, H-bond donor, H-bond acceptor and hydrophobic features of a number of chemical scaffolds included in an in-house library of 5-HT_{1A} ligands. The results coming from Model I and II CoMFA and CoMSIA studies reveal useful suggestions for the further design of new chemical entities, and are also able to predict their affinity and selectivity profiles prior to synthesis.

In particular, despite the fact that the two group compounds showed different conformations and occupation of the 3D-QSAR contour maps, the introduction of lactame and imide decorations attempted only for Group B resulted to be beneficial (also in terms of selectivity) within the whole dataset. This kind of substitution is highly encouraged as well as the choice of a proper flexible linker connecting the terminal aromatic ring with an hydrophobic core enriched with polar and H-bond acceptor functions.

Disclosure statement

The authors declare that they have no conflict of interest.

Funding

This work was financially supported by the University of Genoa.

References

- Hannon J, Hoyer D. Molecular biology of 5-HT receptors. *Behav Brain Res* 2008;195:198–213.
- Yocca FD, Hyslop DK, Smith DW, Maayani S. BMY 7378, a buspirone analog with high affinity, selectivity and low intrinsic activity at the 5-HT_{1A} receptor in rat and guinea pig hippocampal membranes. *Eur J Pharmacol* 1987;137:293–4.
- Olivier B, Soudijn W, van Wijngaarden I. The 5-HT_{1A} receptor and its ligands: structure and function. *Prog Drug Res* 1999;52:103–65.
- Gonzalez LE, File SE, Overstreet DH. Selectively bred lines of rats differ in social interaction and hippocampal 5-HT_{1A} receptor function: a link between anxiety and depression? *Pharmacol Biochem Behav* 1998;59:787–92.
- Gurwitz D. Novel 5-HT-receptor agonists: F11440, MKC242 and BAYx3702. *Drug Discov Today* 1999;4:142–3.
- Schechter LE, Smith DL, Rosenzweig-Lipson S, et al. Lecozotan (SRA-333): a selective serotonin 1A receptor antagonist that enhances the stimulated release of glutamate and acetylcholine in the hippocampus and possesses cognitive-enhancing properties. *J Pharm Exp Ther* 2005;314:1274–89.
- Fiorino F, Severino B, Magli E, et al. 5-HT(1A) receptor: an old target as a new attractive tool in drug discovery from central nervous system to cancer. *J Med Chem* 2014;57:4407–26.
- Patane MA, DiPardo RM, Price RP, et al. Selective alpha-1a adrenergic receptor antagonists. Effects of pharmacophore regio- and stereochemistry on potency and selectivity. *Bioorg Med Chem Lett* 1998;8:2495–500.

9. Brasili L, Sorbi C, Franchini S, et al. 1,3-Dioxolane-based ligands as a novel class of α 1-adrenoceptor antagonists. *J Med Chem* 2013;46:1504–11.
10. Sorbi C, Franchini S, Tait A, et al. 1,3-Dioxolane-based ligands as rigid analogues of naftopidil: structure-affinity/activity relationship at α 1- and 5-HT1A receptors. *ChemMedChem* 2009;4:393–9.
11. Franchini S, Tait A, Prandi A, et al. (2,2-Diphenyl-[1,3]oxathiolan-5-ylmethyl)-(3-phenyl-propyl)-amine a new potent and selective 5-HT1A receptor agonist. *ChemMedChem* 2009;4:196–203.
12. Franchini S, Prandi A, Baraldi A, et al. 1,3-Dioxolane-based ligands incorporating a lactam or imide moiety: structure-affinity/activity relationship at α 1-adrenoceptor subtypes and at 5-HT1A receptors. *Eur J Med Chem* 2010;45:3740–51.
13. Franchini S, Prandi A, Sorbi C, et al. Discovery of a new series of 5-HT1A receptor agonists. *Bioorg Med Chem Lett* 2010;20:2017–20.
14. Prandi A, Franchini S, Manasieva LI, et al. Synthesis, biological evaluation, and docking studies of tetrahydrofuran-cyclopentanone- and cyclopentanol-based ligands acting at adrenergic α - and serotoninine 5-HT1A receptors. *J Med Chem* 2012;55:23–36.
15. Franchini S, Battisti UM, Baraldi A, et al. Structure-affinity/activity relationships of 1,4-dioxo-spiro[4.5]decane based ligands at α 1 and 5-HT1A receptors. *Eur J Med Chem* 2014;87:248–66.
16. Guariento S, Bruno O, Fossa P, Cichero E. New insights into PDE4B inhibitor selectivity: CoMFA analyses and molecular docking studies. *Mol Divers* 2016;20:77–92.
17. Cichero E, Buffa L, Fossa P. 3,4,5-Trisubstituted-1,2,4-4H-triazoles as WT and Y188L mutant HIV-1 non-nucleoside reverse transcriptase inhibitors: docking-based CoMFA and CoMSIA analyses. *J Mol Model* 2011;7:1537–50.
18. Cichero E, Cesarini S, Mosti L, Fossa P. CoMFA and CoMSIA analyses on 1,2,3,4-tetrahydropyrrolo[3,4-b]indole and benzimidazole derivatives as selective CB2 receptor agonists. *J Mol Model* 2010;16:1481–98.
19. Cichero E, Cesarini S, Mosti L, Fossa P. CoMFA and CoMSIA analyses on 4-oxo-1,4-dihydroquinoline and 4-oxo-1,4-dihydro-1,5-, -1,6- and -1,8-naphthyridine derivatives as selective CB2 receptor agonists. *J Mol Model* 2010;16:677–91.
20. Mella-Raipán J, Hernández-Pino S, Morales-Verdejo C, Pessoa-Mahana D. 3D-QSAR/CoMFA-based structure-affinity/selectivity relationships of aminoalkylindoles in the cannabinoid CB1 and CB2 receptors. *Molecules* 2014;19:2842–61.
21. Cichero E, Brullo C, Bruno O, Fossa P. Exhaustive 3D-QSAR analyses as a computational tool to explore the potency and selectivity profiles of thieno[3,2-d]pyrimidin-4(3H)-one derivatives as PDE7 inhibitors. *RSC Adv* 2016;6:61088–108.
22. Mei D, Yin Y, Wua F, et al. Discovery of potent and selective urea-based ROCK inhibitors: exploring the inhibitor's potency and ROCK2/PKA selectivity by 3D-QSAR, molecular docking and molecular dynamics simulations. *Bioorg Med Chem* 2015;23:2505–17.
23. MOE: Chemical Computing Group Inc. Montreal. H3A 2R7 Canada. Available from: www.chemcomp.com.
24. Franchini S, Baraldi A, Sorbi C, et al. Enantiomeric resolution of [(2,2-diphenyl-1,3-dioxolan-4-yl)methyl](2-phenoxyethyl)-amine, a potent α 1 and 5-HT1A receptor ligand: an in vitro and computational study. *Med Chem Commun* 2015;6:677–90.
25. Cramer IIRRD, Patterson DE, Bunce JD. Comparative Molecular Field Analysis (CoMFA). Effect of shape on binding of steroids to carrier proteins. *J Am Chem Soc* 1988;110:5959–67.
26. Klebe G, Abraham U, Mietzner T. Molecular similarity indices in a comparative analysis (CoMSIA) of drug molecules to correlate and predict their biological activity. *J Med Chem* 1994;37:4130–46.
27. Sybyl-X 1.0. Tripos Inc. 1699 South Hanley Road, St Louis, Missouri 63144, USA.
28. Cichero E, Cesarini S, Fossa P, et al. Thiocarbamates as non-nucleoside HIV-1 reverse transcriptase inhibitors: docking-based CoMFA and CoMSIA analyses. *Eur J Med Chem* 2009;44:2059–70.
29. Cichero E, Cesarini S, Fossa P, et al. Acylthiocarbamates as non-nucleoside HIV-1 reverse transcriptase inhibitors: docking studies and ligand-based CoMFA and CoMSIA analyses. *J Mol Model* 2009;15:871–84.
30. Cichero E, Bruno O, Fossa P. Docking-based CoMFA and CoMSIA analyses of tetrahydro- β -carboline derivatives as type-5 phosphodiesterase inhibitors. *J Enzyme Inhib Med Chem* 2011;27:730–43.
31. Partyka A, Chłoń-Rzepa G, Wasik A, et al. Antidepressant and anxiolytic-like activity of 7-phenylpiperazinyllalkyl-1,3-dimethyl-purine-2,6-dione derivatives with diversified 5-HT_{1A} receptor functional profile. *Bioorg Med Chem* 2015;23:212–21.